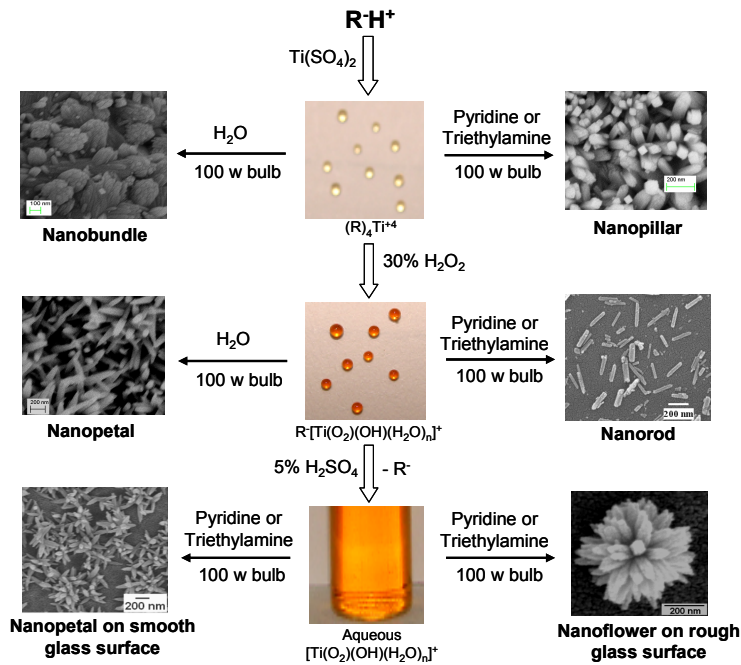


New hydrothermal process for hierarchical TiO_2 nanostructures

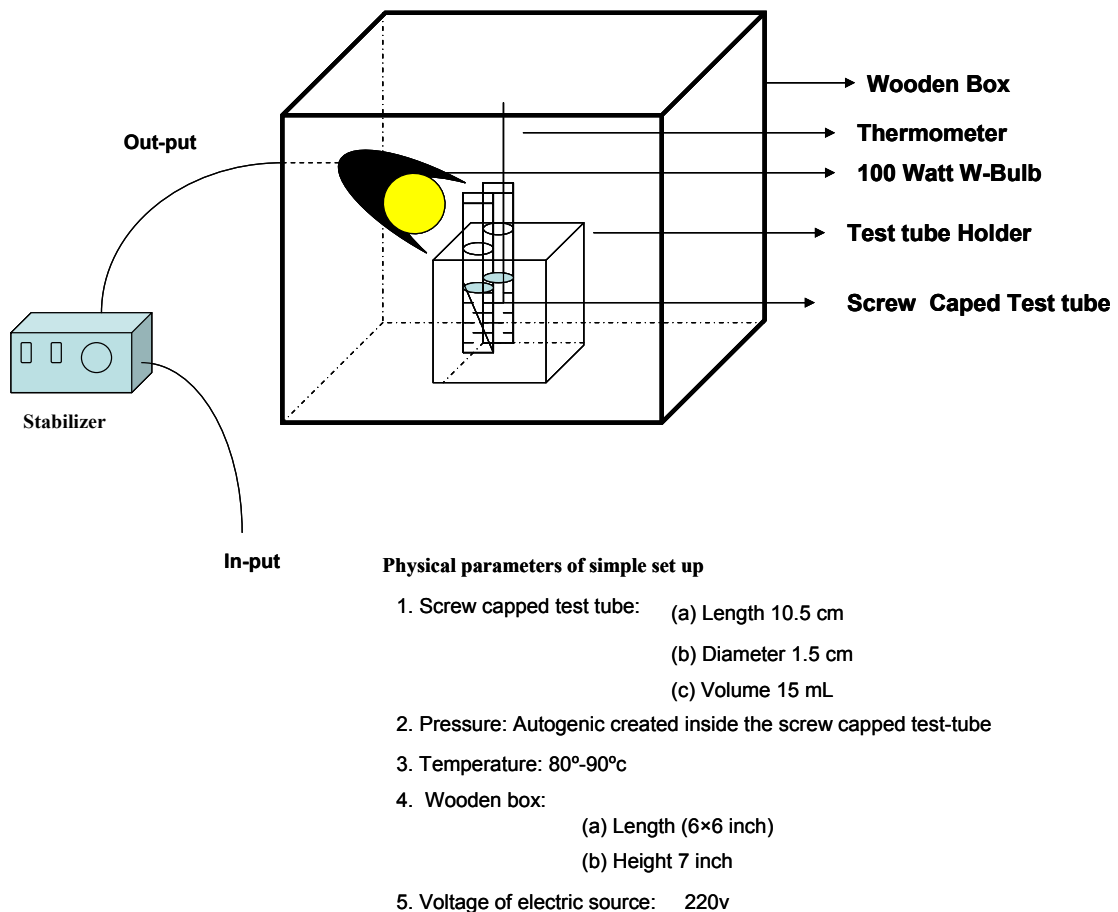
Arun Kumar Sinha, Subhra Jana, Surojit Pande, Sougata Sarkar, Mukul Pradhan,
Mrinmoyee Basu, Sandip Saha, Anjali Pal and Tarasankar Pal*

Electronic Supplementary Information

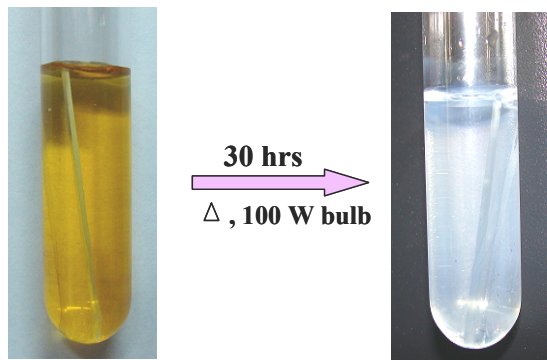
ESI 1 Schematic representation for the formation of different shapes of TiO_2 nanocrystals



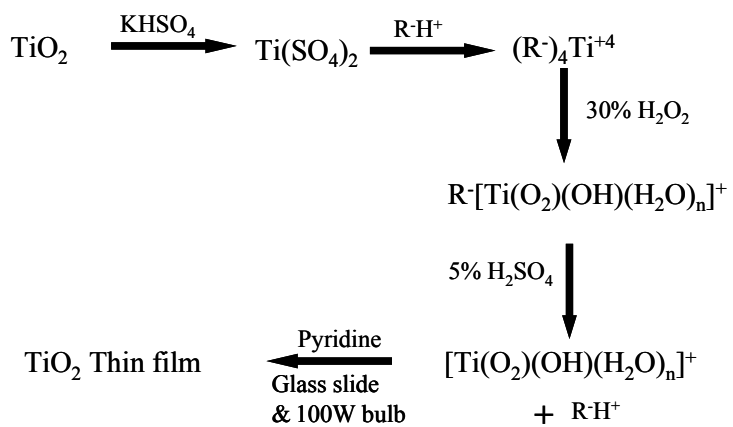
ESI 2 Schematic representation of the set up for hydrothermal (MHT) reaction



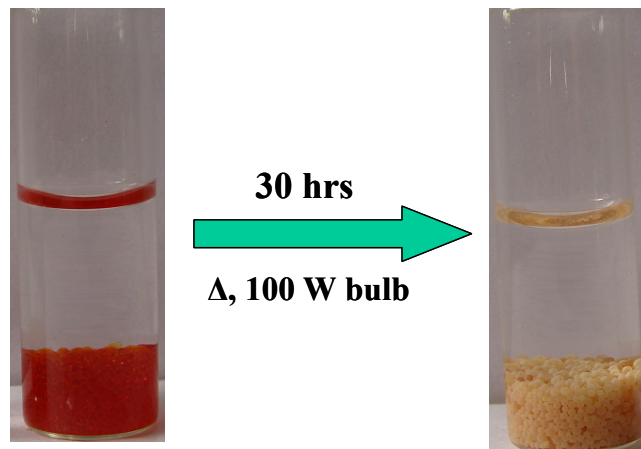
ESI 3 Photograph of TiO_2 nanocrystals formation on glass surface at the air-water interface



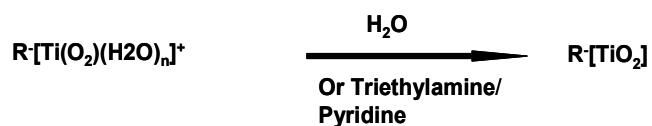
Reaction equation:



ESI 4 Photograph of TiO₂ nanocrystals formation on resin surface at the solid-liquid interface



Reaction equation:



ESI 5 Experimental Section

Materials and instruments

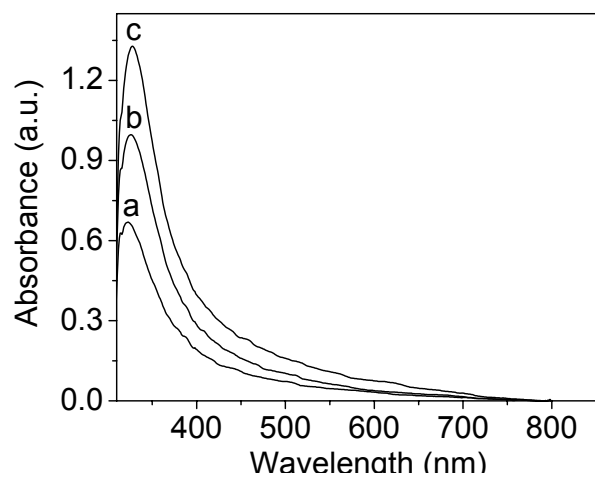
All the reagents were of AR grade. Triple distilled water was used throughout the experiment. Titanium dioxide was obtained from Loba-chemie Indoaustralnal Co. Sulfuric acid was purchased from E-Merck. SERALITE-SRC-120 standard grade strongly cationic exchange resin (ion exchange capacity 4.5 meg/g dry resin), pyridine, triethylamine and KHSO₄ were obtained from Sisco Research Laboratories. Pt crucible was purchased from Sigma Aldrich. All the reagents were used without further purification. Glass slides and screw capped test tube were purchased from Blue Star India Ltd. and were cleaned prior to thin-film formation.

All UV–Visible absorption spectra were recorded in a SPECTRASCAN UV 2600 digital spectrophotometer (Chemito, India). XRD was done in a PW1710 diffractometer, a Philips, Holland, instrument. The XRD data were analyzed using JCPDS software. Raman spectra of TiO₂ nanocrystals were obtained with a Renishaw Raman Microscope, equipped with a He–Ne laser excitation source emitting at a wavelength of 633 nm, and a Peltier cooled (-70 °C) charge coupled device (CCD) camera. A Leica microscope with 20× objective lens was used. The holographic grating with 1800 grooves/mm and the 1 cm⁻¹ slit enabled the spectral resolution. Laser power at the sample was 12 mW and the data acquisition time was 30 sec. FESEM analysis was performed with a supra 40, Carl Zeiss Pvt. Ltd instrument and an EDAX machine (Oxford link and ISIS 300) attached to the instrument was used to obtain the nanocrystal morphology and composition. TEM analysis was performed with an instrument H-9000 NAR, Hitachi, using an accelerating voltage of 300 kV.

Preparation of Ti(SO₄)₂ and Titanium peroxy compound:

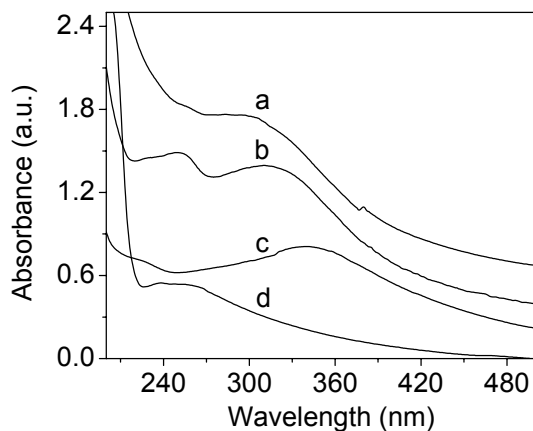
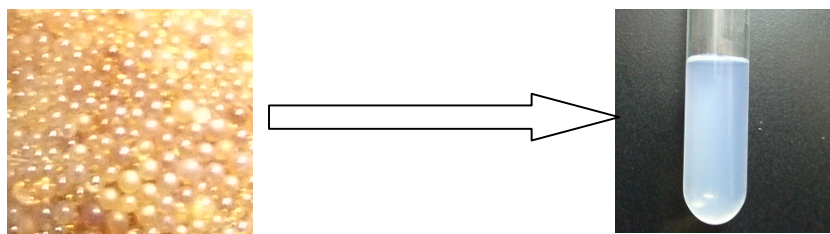
Titanic sulfate was prepared by fusing commercial titanium dioxide powder with ~12 fold excess of KHSO₄. The clear melt was cooled, powdered and was extracted with cold dilute sulfuric acid (5%) and then filtered. Next, titanium(IV) precursor ions (0.58 mM) were allowed to exchange with H⁺ ions of the neat acidic form of the cation-exchange resin beads (R⁻H⁺) with occasional shaking and was kept overnight. The resin beads on which titanium precursor ions were immobilized, were washed several times with water to drain out the un-exchanged Ti(IV) species. Now, 30% H₂O₂ was added to the resin beads and all the resin beads turned orange. Then the orange colored resin beads were washed with copious amount of water for several times to remove excess H₂O₂. Pure titanium peroxy compound (devoid of H₂O₂) was leached out from resin bead with 5% H₂SO₄ and the aqueous solution of peroxy compound was used for MHT reactions.

ESI 6a UV-Visible absorption spectra of TiO₂ nanoflowers as film on quartz slide surface after repetitive (a to c) deposition. The film bearing quartz slides were immersed in the aqueous titanium peroxy solution and were subjected to MHT reaction in presence of pyridine and subsequently analyzed in the spectrophotometer placing the quartz slides in the cuvette



ESI 6b Preparation of colloidal suspension of TiO₂ nanocrystals from resin beads for UV-Visible study

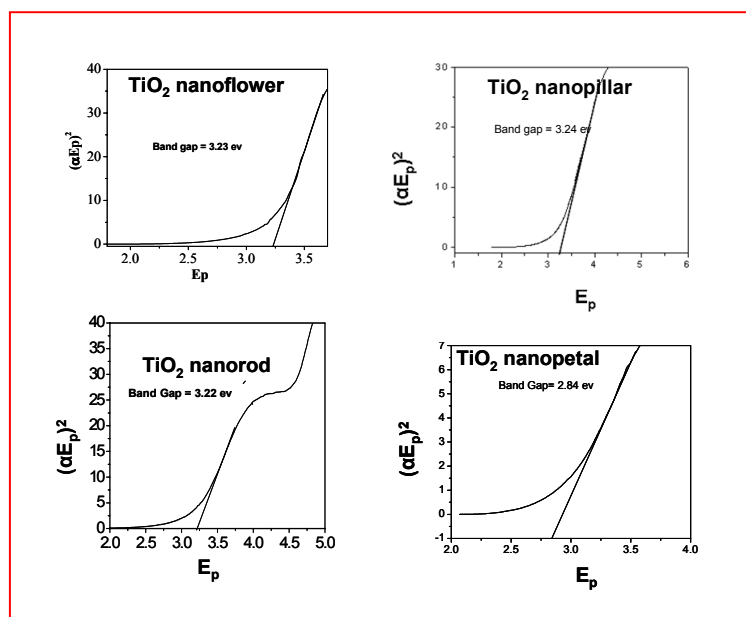
Under sonication (~10 min) TiO₂ nanocrystals leach out in ethanol from the resin beads and form a sol. The sol has been exploited to study the optical property of TiO₂ nanocrystals in suspension by UV-Visible absorption spectroscopy. All absorption spectra were recorded in a Shimadzu UV-160 spectrophotometer (Kyoto, Japan) using a 1 cm quartz cuvette.



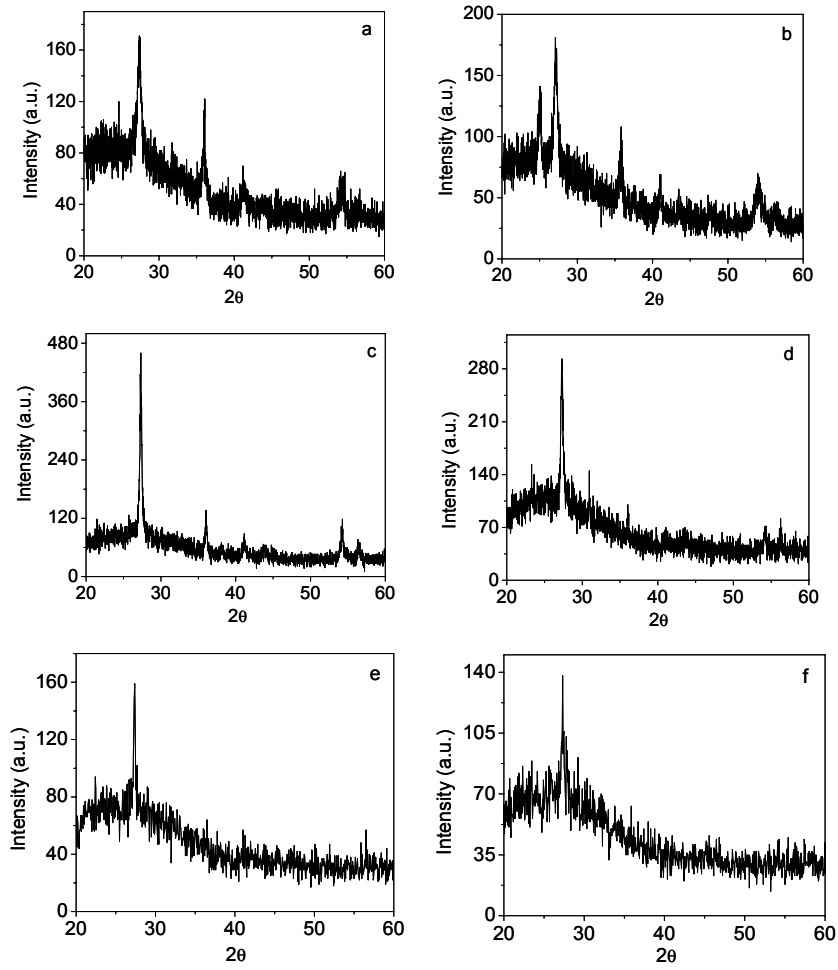
UV-Visible absorption spectra of TiO₂ nanocrystals (a) nanopillars (b) nanorods (c) nanopetals and (d) nanobundles.

ESI 7 Band position and band gap energy value of different TiO₂ nanocrystals

Different shape of TiO ₂ nanocrystal	Band position (nm)	Band gap energy value (eV)
Flower	327	3.23
Pillar	302	3.24
Rod	310	3.22
Petal	342	2.82
Bundle	246	----

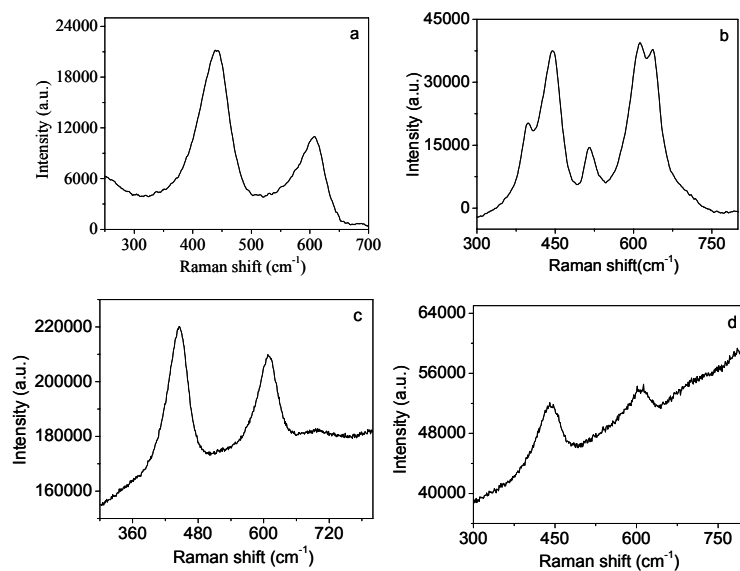


ESI 8 XRD pattern of TiO₂ nanocrystals for (a) flowers (b) flowers after heat treatment at 450 °C (c) rods (d) petals (e) pillars and (f) bundles

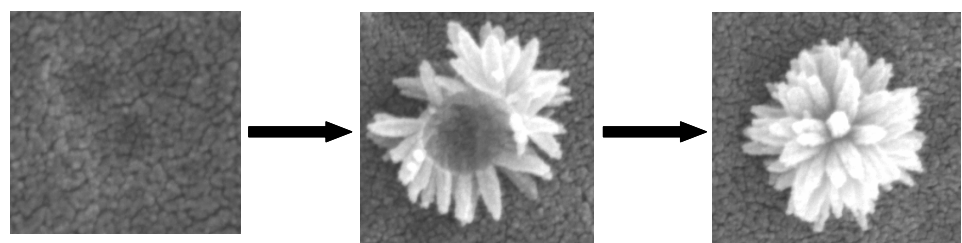


ESI 9 Raman spectra of TiO₂ nanocrystals for (a) flowers (b) flowers at 450 °C (c) rods and (d) petals

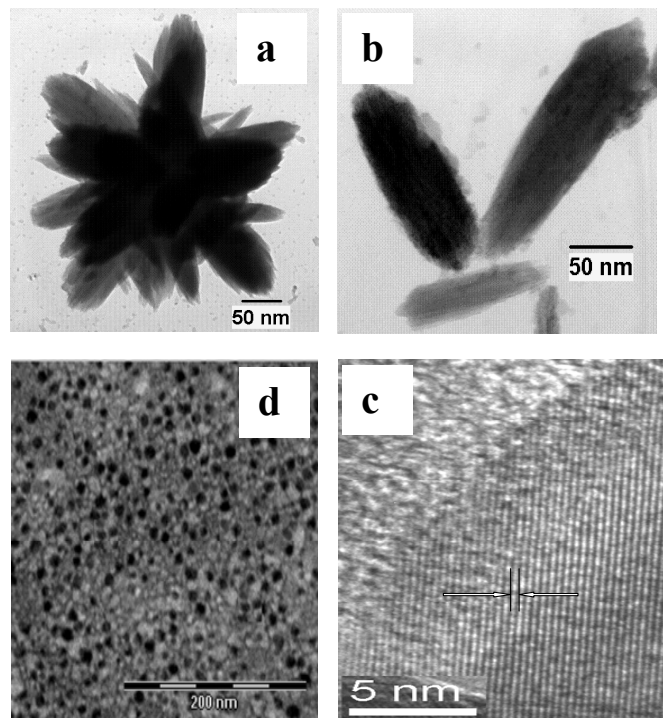
Raman spectroscopy helps us to know the different phases of the as-deposited titania film before and after subsequent heat treatment. Rutile TiO₂ is tetragonal and belongs to D_{4h}¹⁴ point group symmetry. The Raman peaks at 440 (for E_g mode) and 608 cm⁻¹ (for A_{1g} mode) (see the ESI 5a) are attributed to the rutile phase of TiO₂ nanocrystals deposited on glass surface. After subsequent heat treatment at 450 °C for 5 h, the titania nanocrystals produce crystalline anatase phase retaining the signature of the rutile phase. Annealed sample show peaks at 397 and 515 cm⁻¹ which corresponds to the anatase phase of TiO₂ (see the ESI 5b). The Raman peaks at 444 and 607 cm⁻¹ of TiO₂ nanorods and nanopetals, isolated from resin beads by sonication, correspond to rutile phase of TiO₂ nanocrystals (see the ESI 5c, d). Isolated nanobundles and nanopillars do not show any characteristic Raman band. However, the microcrystallinity of TiO₂ nanobundles and nanopillars has been authenticated from XRD analysis.



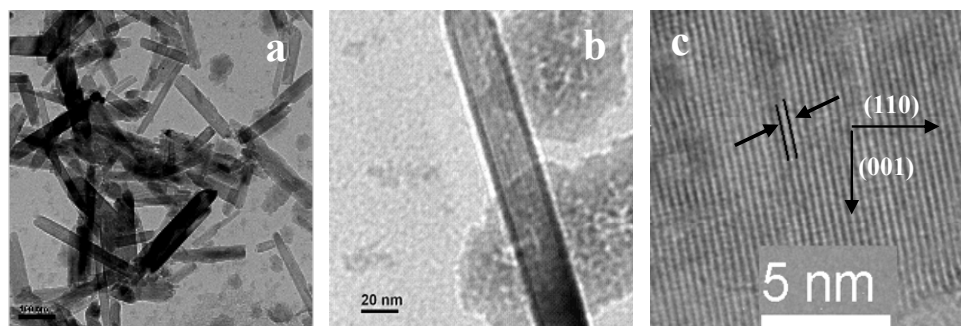
ESI 10 FESEM images to represent the step-wise formation of TiO₂ nanoflowers at the point of surface defect



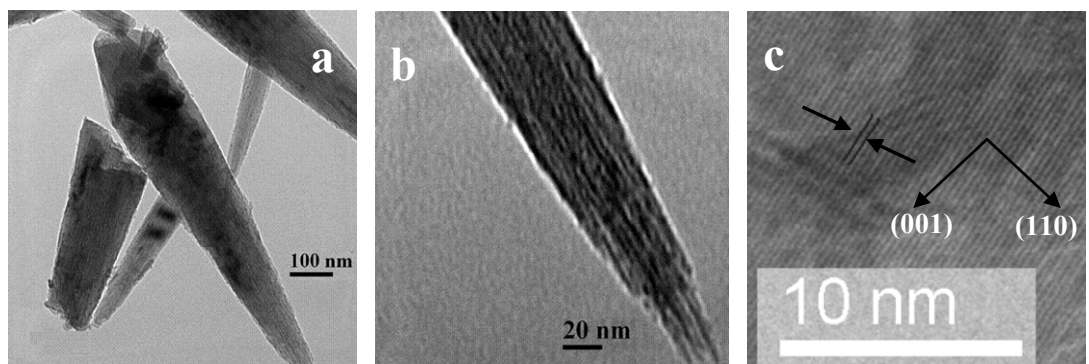
ESI 11 TEM images of (a) nanoflowers (b) nanopetals (c) fringe spacing of TiO_2 nanocrystals on glass surface and (d) spherical nanoparticles of the mother liquor containing the decomposed peroxy compound and pyridine



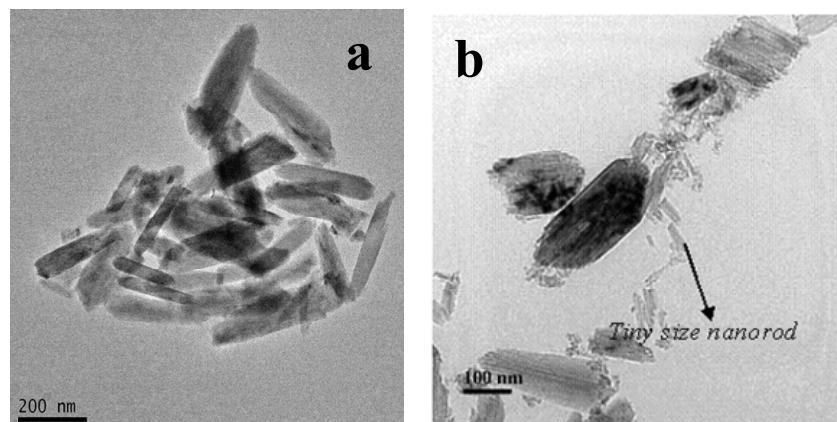
ESI 12 TEM images of TiO_2 nanorods at (a) low magnification (b) high magnification and (c) fringe spacing of TiO_2 nanocrystals on resin surface



ESI 13 (a) TEM (b) HRTEM and (c) fringe spacing of TiO_2 nanopetals on resin surface



ESI 14 TEM images of (a) nanopillars and (b) nanobundles of TiO₂ nanocrystals on resin surface



ESI 15 FESEM image of TiO_2 nanoflowers on glass surface at the point of deliberately created surface defect by HF etching for flower formation

